

Author's Accepted Manuscript

A Langevin model of physical forces in cell volume fluctuations

Steven M Zehnder, Federico M Zegers, Thomas E Angelini



PII: S0021-9290(16)00009-9
DOI: <http://dx.doi.org/10.1016/j.jbiomech.2015.12.051>
Reference: BM7519

To appear in: *Journal of Biomechanics*

Received date: 6 July 2015
Revised date: 30 October 2015
Accepted date: 30 December 2015

Cite this article as: Steven M Zehnder, Federico M Zegers and Thomas E Angelini, A Langevin model of physical forces in cell volume fluctuations *Journal of Biomechanics*, <http://dx.doi.org/10.1016/j.jbiomech.2015.12.051>

This is a PDF file of an unedited manuscript that has been accepted for publication. As a service to our customers we are providing this early version of the manuscript. The manuscript will undergo copyediting, typesetting, and a review of the resulting galley proof before it is published in its final citable form. Please note that during the production process errors may be discovered which could affect the content, and all legal disclaimers that apply to the journal pertain

1 **A Langevin model of physical forces in cell volume fluctuations**

2 Steven M Zehnder¹, Federico M Zegers^{1,2}, Thomas E Angelini^{1,3,4*}

3 ¹ Department of Mechanical and Aerospace Engineering, University of Florida, Gainesville,
4 USA

5 ² Department of Mathematics, University of Florida, Gainesville, USA

6 ³ J. Crayton Pruitt Family Department of Biomedical Engineering, University of Florida,
7 Gainesville, USA

8 ⁴ Institute of Cell and Regenerative Medicine, University of Florida, Gainesville, USA

9 * Correspondence to: Tel: +13523926438, Fax: +13523927303,

10 Email address: t.e.angelini@ufl.edu (T. E. Angelini)

11

12 **Cells interact mechanically with their physical surroundings by attaching to the**
13 **extracellular matrix or other cells and contracting the cytoskeleton. Cells do so**
14 **dynamically, exhibiting fluctuating contractile motion in time. In monolayers, these**
15 **dynamic contractions manifest as volume fluctuations, which involve the transport of fluid**
16 **in and out of the cell. An integrated understanding of cell elasticity, actively generated**
17 **stresses, and fluid transport has not yet been developed. Here we apply a minimal model of**
18 **these forces to cell volume fluctuation data, elucidating the dynamic behavior of cells**
19 **within monolayers.**

20

21 **Introduction**

22 In each type of tissue throughout the body, cells generate forces to sense the rigidity of
23 their surroundings; cell function, fate, and survival depend on the cellular mechanical
24 microenvironment (Discher et al., 2005; Harris et al., 1980; Pelham and Wang, 1997). The cell's
25 F-actin cytoskeleton comprises several types of contractile elements that actively exert forces on
26 the extracellular matrix and on neighboring cells. On surfaces, cells form stress fibers that
27 generate traction forces (Dembo and Wang, 1999; Pelham and Wang, 1997). In monolayers,
28 cells form equatorial actin belts that contract to generate in-plane tensile forces (Hirano et al.,
29 1987; Parczyk et al., 1989; Schroeder, 1973). Across the cell surface, a cortical actin network

30 contracts to augment membrane tension and rigidity (Engler et al., 2006; Zhelev et al., 1994). An
31 F-actin network links the apical and basolateral cell surfaces, permeates much of the cell volume,
32 and contracts to generate cytoskeletal pre-stress, modulating the stiffness of the cell itself (Wang
33 et al., 2002). If cells maintain a state of mechanical equilibrium, internal elements that bear
34 compressive loads or stresses in the extracellular surroundings must balance these tensions.
35 Internally, tension may be balanced by microtubules, which exhibit a buckling instability like
36 slender rods under compression (Brangwynne et al., 2006). Externally, deformations in the cell's
37 substrate and stresses in neighboring cells could balance the cell generated tension (Tambe et al.,
38 2011; Treppe et al., 2009).

39 The collective migration patterns and transient stress fluctuations that exist within
40 monolayers indicate that internally generated tensile forces within each cell are not balanced by
41 elastic forces in their surroundings (Tambe et al., 2011). Imbalances in normal stress may drive
42 the volumetric expansion or contraction of cells; it was recently shown in these dynamic
43 monolayers that cells fluctuate in volume by 20% every four hours (Zehnder et al., 2015). Such
44 volume fluctuations are facilitated by the cell's permeability; water from the cytosol can
45 exchange with the surrounding bath or between neighboring cells through gap junctions with
46 about the same hydraulic resistance (Bennett and Verselis, 1992; Giaume et al., 1986; Hoffmann
47 et al., 2009; Timbs and Spring, 1996; Zehnder et al., 2015). The interplay between a minimal
48 number of dominant forces like cell elasticity, resistance to fluid transport, and cell generated
49 stress may determine volume fluctuations of single cells. However, this integrated set of
50 physical forces that control cell volume fluctuations have not been investigated previously.

51 Here we explore the mechanics of spontaneous cell volume fluctuations in Madin Darby
52 Canine Kidney (MDCK) epithelial monolayers. The sizes of over 1000 cells are measured and

53 tracked over time. We fit a simple damped harmonic oscillator model driven by a random white
54 noise stress to the average power spectrum of cell volume fluctuations, determining the
55 corresponding elastic and viscous parameters. We also use the fits to estimate the amplitude of
56 the driving stress, finding a value of 6.8 kPa. These results introduce a potential method for
57 measuring stresses and stiffness of cells grown on rigid surfaces like glass and polystyrene, on
58 which soft substrate methods like traction force microscopy cannot be employed.

59 **Materials and Methods**

60 Madin Darby Canine kidney cells with green fluorescent protein (GFP) labelled histones
61 are cultured in Duplecco's Modified Eagle's Medium (DMEM) supplemented with 10% fetal
62 bovine serum and 1% penicillin streptomycin. Histones are tagged with the triple nuclear
63 localization signal (NLS) expression system and a gentamicin resistance sequence for cell
64 selection. Culture medium is supplemented with 0.5 $\mu\text{g}/\text{mL}$ gentamicin to continuously select for
65 cells with fluorescent histones. Cells are incubated at 37 °C under a 5% CO₂ atmosphere. Prior to
66 imaging, cells are seeded in 5mm diameter islands at a minimally confluent density on glass-
67 bottomed petri dishes coated with bovine collagen type I. Dishes are imaged on an inverted light
68 microscope with an environmental control stage maintained at 37 °C in a 5% CO₂ atmosphere.
69 Phase contrast and FITC fluorescence images are captured in time-lapse every minute over the
70 course of 9 hours. Exposure times are kept below 100 ms per minute and fluorescence excitation
71 light is passed through a 10% transmitting neutral density filter to limit light exposure.

72 **Results**

73 We track cell positions by following fluorescent nuclei in space and time, and at each time
74 point we compute a Voronoi tessellation map from the cell centers. The area of each cell within

75 the continuous layer is estimated from the area of its corresponding Voronoi cell. In our
 76 previous work we showed that cell volume fluctuations are proportional to the fluctuations in this
 77 projected cell area (Zehnder et al., 2015). Thus, the volume fluctuation of each cell in time is
 78 defined by projected area fluctuations, given by $\delta V(t) = [A(t) - \langle A \rangle_t] / s_A$, where $A(t)$ is the
 79 projected area of a cell at any point in time, $\langle A \rangle_t$ is that cell's average area and s_A is the standard
 80 deviation of area over time. This definition of volume fluctuation is chosen to compute a
 81 normalized cell volume autocorrelation function, $C_{\delta V - \delta V}(\tau)$, which exhibits a characteristic
 82 oscillation time of approximately 4 hours, consistent with individual traces of cell volume
 83 (Zehnder et al., 2015) (Fig. 1). Errors associated with determining cell centers by their nuclei
 84 rather than from their geometric centers do not affect the analysis performed here; the results do
 85 not depend on translocation of the whole cell. However, direct measurement of volume
 86 fluctuations from the borders of over 300 cells shows that the Voronoi treatment of the cell as
 87 polygonal artificially reduces the measured amplitude of cell volume fluctuations, which we
 88 discuss further below.

89 To analyze cell volume fluctuations with a minimal physics-based model, we compute
 90 the power spectral density function, $S_{\delta V - \delta V}(\omega)$, by Fourier transforming $C_{\delta V - \delta V}(\tau)$. The peaked
 91 nature of the power spectrum and oscillatory nature of the correlation function are reminiscent of
 92 the behavior of a simple damped harmonic oscillator (DHO). We therefore model cell volume
 93 fluctuations with a Langevin equation in terms of normal stress and strain, given by

$$c_1 \gamma_V(t) + c_2 \dot{\gamma}_V(t) + c_3 \ddot{\gamma}_V(t) = \sigma_N(t), \quad (1)$$

94 where c_1, c_2, c_3 are unknown constants and $\gamma_V(t)$ is volumetric strain defined as

95 $\gamma_V(t) = [V(t) - \langle V \rangle_t] / \langle V \rangle_t$. $\sigma_N(t)$ is assumed to be a random white noise driving stress with

96 amplitude σ_0 . Thus, $\sigma_N = \sigma_0 f(t)$, where $f(t)$ is a delta-correlated random noise function with a
 97 constant power spectrum equal to unity, and all other terms are treated as passive mechanical
 98 responses to the driving stress. Traditionally, Langevin equations are used to incorporate the
 99 effects of random forces from Brownian solvent particles in transport equations; modern
 100 Langevin treatments model stochastic driving forces in active systems including bacteria, self-
 101 driven colloids, tissue cells, and the cytoskeleton (Marchetti et al., 2013). Here we consider the
 102 random driving stress, $\sigma_N(t)$, to be generated by stochastic contractions and relaxations of
 103 molecular motors on the cytoskeleton (Guo et al., 2014).

104 In equation 1, c_1 is the elastic modulus of a cell associated with volumetric strain. The
 105 molecular liquid component of the cytosol does not compress in these volume fluctuations, so c_2
 106 is the drag coefficient associated with moving water into and out of cells which we have
 107 previously shown can occur by transport across the membrane or through gap junctions (Zehnder
 108 et al., 2015). When a cell expands or contracts within a confluent monolayer, all of the
 109 surrounding cells must move, on average, 180° out of phase with the central individual cell,
 110 expanding when the cell contracts and contracting when the cell expands. To capture the
 111 mechanical signals associated with this complementary motion, we include the term $c_3 \ddot{\gamma}_V(t)$,
 112 which is analogous to an inertial term. However, at the extremely slow rates of oscillation, inertia
 113 is totally negligible; this term merely approximates the out of phase chemo-mechanical signals in
 114 a cell's surroundings.

115 We rewrite equation 1 in terms of σ_0 and $\delta V(t)$ yielding

$$c_1 \delta V(t) + c_2 \dot{\delta V}(t) + c_3 \ddot{\delta V}(t) = \frac{\langle V \rangle_t}{s_V} \sigma_0 f(t). \quad (2)$$

116 With the equation of motion in terms of $\delta V(t)$ we define our model spectrum,

$$S_{\delta V-\delta V}(\omega) = \delta V(\omega) \delta V^*(\omega), \quad (3)$$

117 where ω is angular frequency, \sim denotes the Fourier transform, and $*$ denotes the complex
 118 conjugate. Taking the Fourier transform of both sides of equation 2 and rearranging terms yields

$$\delta V(\omega)(c_1 + i\omega c_2 - \omega^2 c_3) = \frac{\langle V \rangle_t}{s_V} \sigma_o f. \quad (4)$$

119 Solving for δV in equation 4 and combining constants into common terms we compute the
 120 classic model power spectral density function of a damped harmonic oscillator,

$$S(\omega) = \frac{A}{(\omega_o^2 - \omega^2)^2 + \omega^2 \Gamma^2} \quad (5)$$

121 where $A = (\langle V \rangle_t \sigma_o / s_V c_3)^2 f f^*$, $\omega_o = \sqrt{c_1/c_3}$, and $\Gamma = c_2/c_3$. We fit the model in equation 5 to
 122 the spectrum determined from the volume fluctuation data, allowing A , ω_o , and Γ to freely vary
 123 using a non-linear least squares algorithm. The fit matches the data over a range denoted by the
 124 blue line in Figure 2A with an R^2 value of 0.99 (Fig 2 A). We find $A = 521 \pm 45 \text{ h}^{-2}$, $\omega_o = 3.1 \pm$
 125 0.1 h^{-1} , and $\Gamma = 12.6 \pm 0.6 \text{ h}^{-1}$. We have also fit other model spectra to the data, in which each
 126 individual term or multiple terms in the equation (1) are dropped. All such candidate models fail
 127 to capture the experimental spectral line-shape and always predict power spectra that decay with
 128 the incorrect power.

129 To estimate each of the model parameters from the three fitting parameters, we relate c_2
 130 to the hydraulic permeability of MDCK cells, $k = 0.06 \mu\text{m}^3 \text{ kPa}^{-1} \text{ s}^{-1}$. (Zehnder et al., 2015). c_2 is
 131 the stress per-unit strain-rate dissipated in volume fluctuations; k is the volumetric flow rate per
 132 unit applied stress. Either of these two parameters can be used in different forms of Darcy's law
 133 to describe the relationship between flow an pressure. The parameters are related by

$$c_2 = \frac{\langle V \rangle_t}{k}. \quad (6)$$

134 We find $c_2 = 22.7$ kPa h. With this estimate of c_2 , all of the other model parameters can be found.
 135 c_3 is determined by $\Gamma = c_2/c_3$, yielding $c_3 = 1.3$ kPa h². From ω_0 and c_3 we determine the
 136 volumetric elasticity of cells, $c_1 = 11.3$ kPa. Finally, we compute the amplitude of the driving
 137 stress, $\sigma_0 = 6.8$ kPa, determined from A and the other parameters already determined. The
 138 method of approximating individual cell volume fluctuations from Voronoi maps is found to
 139 under-estimate the amplitude of fluctuations by about 17%, which correspondingly decreases this
 140 estimate of σ_0 . Experimental measurement of cell permeability, k , will allow confidence intervals
 141 to be generated for all of the model parameters estimated here.

142

143 **Discussion and Conclusions**

144 In this study we have applied a minimal physical model to experimental data of cell
 145 volume fluctuations. We have characterized the line-shape of the fluctuation spectrum and
 146 determined the physical parameters that control cell volume fluctuations and cell-cell mechanical
 147 interactions. We find that cell volume fluctuations are well characterized by a simple damped
 148 harmonic oscillator spectrum that deviates from the data at low frequencies. The simplest
 149 explanation of this deviation is that the cytoskeletal contractions driven by molecular motors and
 150 ATP hydrolysis cannot generate a white noise spectrum over time-scales of hours. Inspired by
 151 studies of the driving spectra of molecular motors in active cytoskeleton networks, we divide the
 152 experimental spectrum by the extrapolated white-noise driven spectrum to estimate the real
 153 driving spectrum (Fig. 2B) (Mizuno et al., 2007). The resulting driving spectrum is high-pass
 154 white noise, which reflects the fact that cells do not expand and contract for periods of time

155 longer than a few hours. This result shows that cell volume oscillations need not arise from a
156 single sinusoidal driving force; a white noise spectrum with a low-frequency cut-off can drive
157 cell volume fluctuations. Further exploration of this potential driving spectrum must be
158 performed by a combination of active measurements that physically drive cell volume
159 fluctuations, and passive measurements like those investigated here.

160 Our results represent a potential method for measuring cell generated stress on rigid
161 substrates like glass. Traction force microscopy is a powerful method that enables the estimation
162 of cell generated forces by measuring how cells deform their substrates (Dembo and Wang,
163 1999). Traction force microscopy cannot be performed on tissue culture polystyrene or
164 functionalized glass surfaces because cells cannot deform these rigid materials. Here, by
165 measuring cell volume fluctuations and estimating a hydraulic permeability for fluid transport,
166 we have measured metrics of cell stiffness and cell generated stress. Experiments that actively
167 indent cell layers and measure both forces and fluid displacement are needed to better determine
168 cell permeability, which anchors the mechanical parameters inferred from our model. The
169 volumetric modulus found here of 11.3 kPa, and the driving stress of 6.8 kPa, are about an order
170 of magnitude larger than moduli and stresses found from cells grown on soft substrates (Tambe
171 et al., 2011; Wang et al., 2002). However, cells grown on stiff substrates are known to exhibit a
172 higher modulus, and the modulus typically measured is a shear modulus which will be smaller
173 than a bulk modulus associated with volume changes (Discher et al., 2005). A combination of the
174 method presented here and traction force microscopy could deepen our understanding of cell
175 mechanics by accounting for resistive forces associated with fluid transport while expanding
176 measurements to include the dynamic behavior of cells.

177 **Conflict of interest**

178 The authors report no conflict of interest

179 **Acknowledgements**

180 We would like to thank Adrian Pegararo for providing transfected MDCK cells expressing GFP
181 labelled histones. This project was funded by NSF grant No. CMMI-1161967.

182 **References**

- 183 Bennett, M., Verselis, V., Year Biophysics of gap junctions. In Seminars in cell biology.
184
- 185 Brangwynne, C.P., MacKintosh, F.C., Kumar, S., Geisse, N.A., Talbot, J., Mahadevan, L., Parker, K.K.,
186 Ingber, D.E., Weitz, D.A., 2006. Microtubules can bear enhanced compressive loads in living cells
187 because of lateral reinforcement. *The Journal of Cell Biology* 173, 733-741.
188
- 189 Dembo, M., Wang, Y.-L., 1999. Stresses at the cell-to-substrate interface during locomotion of
190 fibroblasts. *Biophysical journal* 76, 2307-2316.
191
- 192 Discher, D.E., Janmey, P., Wang, Y.-L., 2005. Tissue Cells Feel and Respond to the Stiffness of Their
193 Substrate. *Science* 310, 1139-1143.
194
- 195 Engler, A.J., Sen, S., Sweeney, H.L., Discher, D.E., 2006. Matrix Elasticity Directs Stem Cell Lineage
196 Specification. *Cell* 126, 677-689.
197
- 198 Giaume, C., Sahuquillo, C., Louvard, D., Korn, H., 1986. Evidence for ionic coupling between MDCK
199 cells at non-confluent and confluent stages of culture. *Biology of the Cell* 57, 33-38.
200
- 201 Guo, M., Ehrlicher, A.J., Jensen, M.H., Renz, M., Moore, J.R., Goldman, R.D., Lippincott-Schwartz, J.,
202 Mackintosh, F.C., Weitz, D.A., 2014. Probing the stochastic, motor-driven properties of the cytoplasm
203 using force spectrum microscopy. *Cell* 158, 822-832.
204
- 205 Harris, A., Wild, P., Stopak, D., 1980. Silicone rubber substrata: a new wrinkle in the study of cell
206 locomotion. *Science* 208, 177-179.
207
- 208 Hirano, S., Nose, A., Hatta, K., Kawakami, A., Takeichi, M., 1987. Calcium-dependent cell-cell adhesion
209 molecules (cadherins): subclass specificities and possible involvement of actin bundles. *The Journal of*
210 *cell biology* 105, 2501-2510.
211
- 212 Hoffmann, E.K., Lambert, I.H., Pedersen, S.F., 2009. Physiology of cell volume regulation in vertebrates.
213 *Physiological reviews* 89, 193-277.
214
- 214 Mizuno, D., Tardin, C., Schmidt, C., MacKintosh, F., 2007. Nonequilibrium mechanics of active
215 cytoskeletal networks. *Science* 315, 370-373.
216
- 217 Marchetti, M.C., Joanny, J.F., Ramaswamy, S., Liverpool, T.B., Prost, J., Rao, M., Aditi Simha, R., 2013.
218 Hydrodynamics of soft active matter. *Reviews of Modern Physics*, 85, 1143-1189.
219

- 220 Parczyk, K., Haase, W., Kondor-Koch, C., 1989. Microtubules are involved in the secretion of proteins at
 221 the apical cell surface of the polarized epithelial cell, Madin-Darby canine kidney. *Journal of Biological*
 222 *Chemistry* 264, 16837-16846.
- 223
- 224 Pelham, R.J., Wang, Y.-l., 1997. Cell locomotion and focal adhesions are regulated by
 225 substrate flexibility. *Proceedings of the National Academy of Sciences* 94, 13661-13665.
- 226 Schroeder, T.E., 1973. Cell Constriction: Contractile Role of Microfilaments in Division and
 227 Development. *American Zoologist* 13, 949-960.
- 228
- 229 Tambe, D.T., Corey Hardin, C., Angelini, T.E., Rajendran, K., Park, C.Y., Serra-Picamal, X., Zhou, E.H.,
 230 Zaman, M.H., Butler, J.P., Weitz, D.A., Fredberg, J.J., Trepap, X., 2011. Collective cell guidance by
 231 cooperative intercellular forces. *Nat Mater* 10, 469-475.
- 232
- 233 Timbs, M., Spring, K., 1996. Hydraulic properties of MDCK cell epithelium. *The Journal of membrane*
 234 *biology* 153, 1-11.
- 235
- 236 Trepap, X., Wasserman, M.R., Angelini, T.E., Millet, E., Weitz, D.A., Butler, J.P., Fredberg, J.J., 2009.
 237 Physical forces during collective cell migration. *Nat Phys* 5, 426-430.
- 238
- 239 Wang, N., Tolić-Nørrelykke, I.M., Chen, J., Mijailovich, S.M., Butler, J.P., Fredberg, J.J., Stamenović,
 240 D., 2002. Cell prestress. I. Stiffness and prestress are closely associated in adherent contractile cells.
 241 *American Journal of Physiology - Cell Physiology* 282, C606-C616.
- 242
- 243 Zehnder, S.M., Suaris, M., Bellaire, M.M., Angelini, T.E., 2015. Cell Volume Fluctuations in MDCK
 244 Monolayers. *Biophysical journal* 108, 247-250.
- 245
- 246 Zhelev, D.V., Needham, D., Hochmuth, R.M., 1994. Role of the membrane cortex in neutrophil
 247 deformation in small pipets. *Biophysical Journal* 67, 696-705.

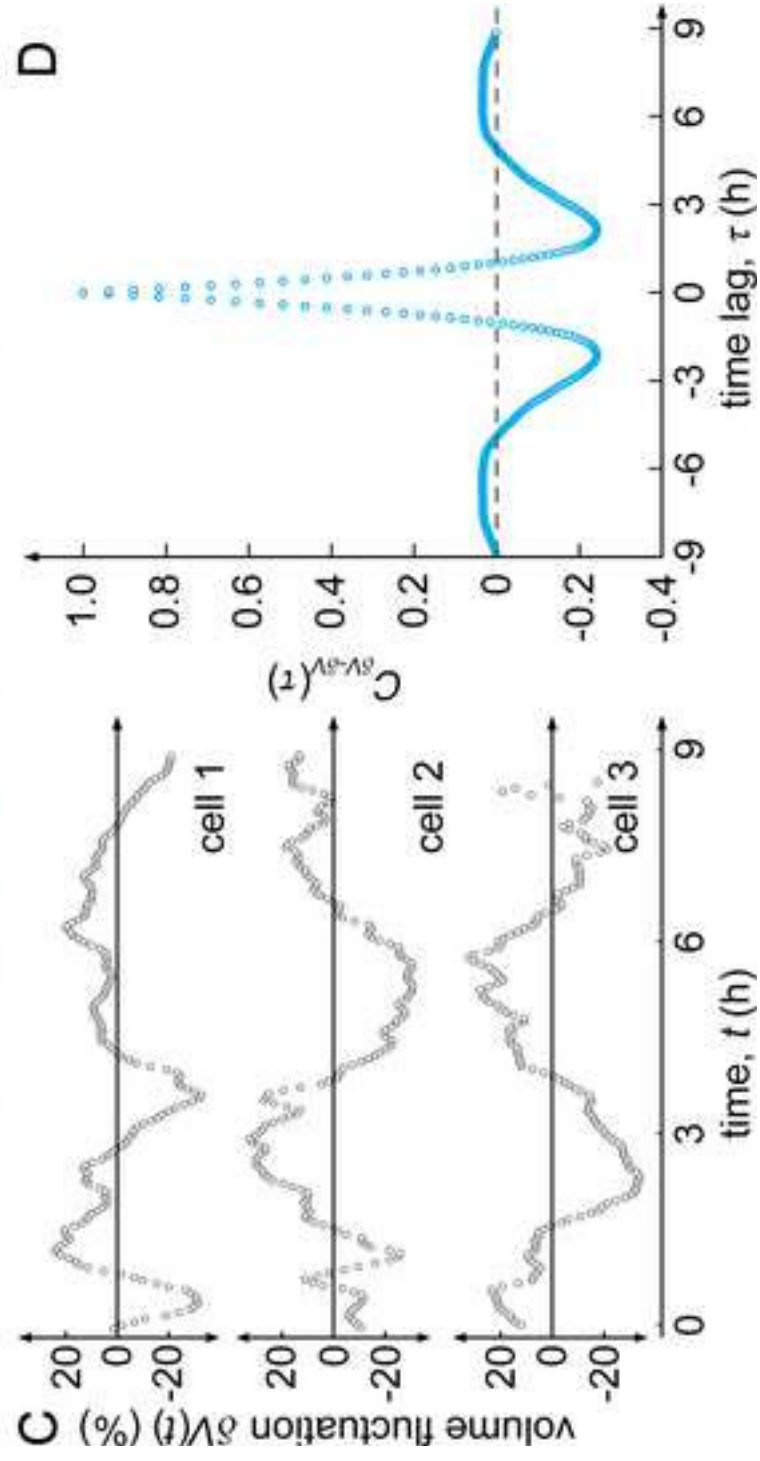
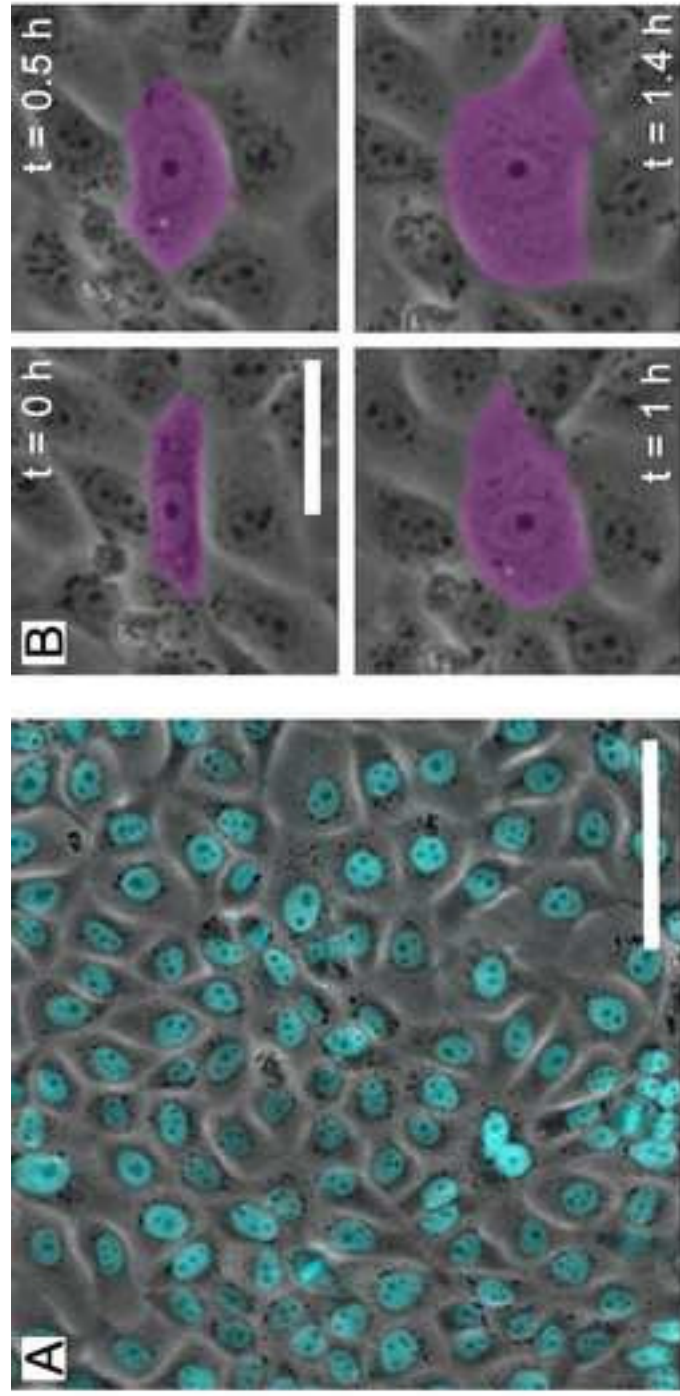
248 Captions

249 **Figure 1.** Cell volume fluctuations. A) Fluorescent nuclei of MDCK epithelial cells are tracked
 250 in time and space. B) Cell sizes can change significantly over short periods of time. C) Individual
 251 traces of cell volume over time for three representative cells show a representative period of
 252 between 4 and 6 hours. D) The volume-volume correlation function averaged over all cells, $C_{\delta V}$
 253 δV , shows an anti-correlation peak at approximately 2 hours, suggesting a 4 hour period of
 254 oscillation ($N=1038$) The gray dotted line denotes zero correlation.

255 **Figure 2.** A damped harmonic oscillator model is fit to the power spectrum of volume
 256 fluctuations. A) The power spectral density function for cell volume fluctuations (data = open
 257 black circles). The blue line represents the fit of the data with the power spectrum model
 258 described in equation 5. The red line is an extension of the model beyond fitted data points. B)
 259 The rescaled spectrum of the driving stress shows a cut-off of the high frequency noise. The red
 260 line denotes $\sigma_o = 6.8$ kPa.

261

262



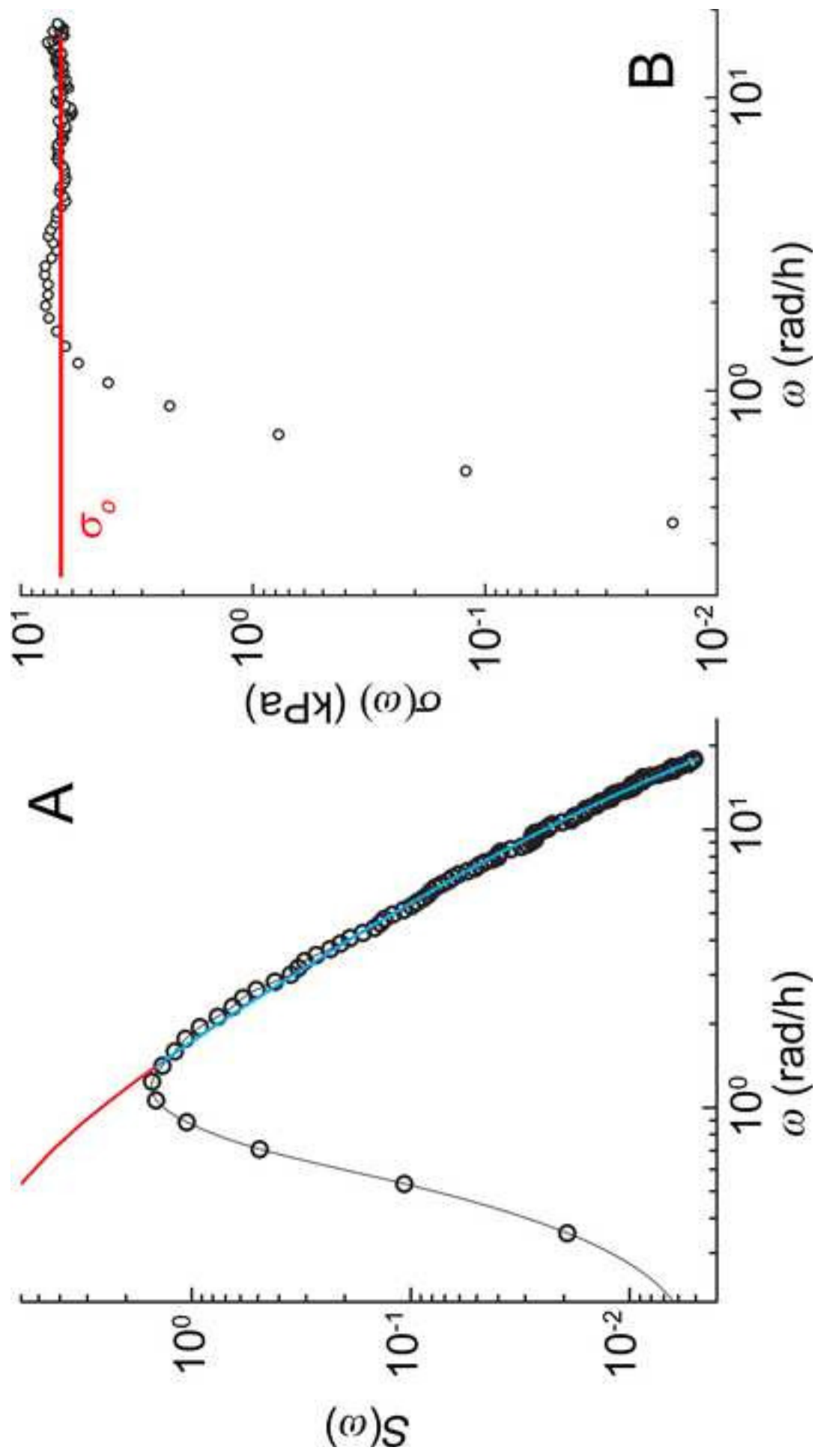


Figure 2